Nanowire Solar Cells

DOI: 10.1002/anie.201006617

Understanding the Origin of the Low Performance of Chemically Grown Silicon Nanowires for Solar Energy Conversion**

*Guangbi Yuan, Kenneth Aruda, Sa Zhou, Andrew Levine, Jin Xie, and Dunwei Wang**

Silicon nanowires (SiNWs) have been proposed as promising candidates for efficient solar energy conversion for at least three reasons: 1) the abundance of elemental Si and the rich knowledge of its electronic and photoelectronic properties, 2) the appeal of the nanowire morphology for improved charge collection, and 3) the widely available synthetic methods that can produce vertically aligned or randomly oriented high-quality SiNWs.[1–5] Despite intense efforts, however, the performance of SiNW-based solar cells remains significantly lower than what has been achieved for bulk Si or micrometer-scale wires.[6–15] The gap between the predicted performance and the inability to deliver raises an important question with regard to the origin of this problem. Owing to the similarity between the science of SiNWs and that of nanowires of many other compositions, finding answers to this question is of great importance to using these materials for efficient solar energy harvesting.[2,5] We performed a detailed study of SiNW electronic properties, which is aimed at understanding what limits the performance of SiNWs, by using electrochemical techniques. Our results reveal that the poor performance is not a result of the nanowire morphology, but is intrinsic to the growth chemistry. The finding suggests that more attention should be paid to the optimization of the synthesis of SiNWs in order to actualize the full potential of this exciting material for energy conversion purposes.

Previous studies have shown that the high surface-to-volume ratio exhibited by SiNWs may be deleterious in reducing open circuit voltages.[1,16] This disadvantage can be partially compensated by gains in short-circuit current caused by the relaxation of charge diffusion distance requirements and improved light absorption;[1,7,14,17–19] energy conversion efficiencies similar to that of bulk-Si-based devices are predicted. However, experimental efforts have failed to meet the expectation (Table 1), thus leaving important questions unanswered, such as whether the nanowire morphology is intrinsically disadvantaged and where research should be focused on.

Table 1: Overview of representative reports on SiNW- or micrometer-sized-wire-based solar energy conversion.

Material	Method	Device	η [%]	Reference
SiNW	CVD	solid[a]	1.80	[14]
SiNW[b]	CVD	solid	3.40	[6]
SiNW	DRIE[c]	solid	5.30	[19]
SiNW/Pt[d]	EE	PEC	8.14	[22]
Si wire[e]	CVD	PEC	3.60	[15]
Si wire	CVD	solid	7.92	[8]

[a] p–n or p–i–n junction solid state devices. [b] Experiment performed on a single nanowire. [c] Deep reactive ion etching. [d] Pt served as catalyst, electrolyte: Br^-/Br_2 in H_2O. [e] Wire diameter: 1.6 μm, wire length: 100 μm; electrolyte: methyl viologen ($MV^{2+/+}$) in H_2O. Although $\eta > 10\%$ has been measured by Zhu et al. (Ref. [20]), an axial p–n junction similar to conventional solar cells was employed. For a fair comparison, the respective reference is not included in the table.

The first question we seek to answer experimentally is whether the nanowire morphology is intrinsically disadvantageous. We compared three types of samples: planar Si wafers, SiNWs prepared by electroless etching,[13,20–22] and SiNWs synthesized by a bottom-up chemical method.[23] Derived from planar Si crystals, electroless etched (EE) SiNWs have the same crystallography and doping level as Si crystals from the bulk, they differ only in the surface-to-volume ratio. Studying EE SiNWs allows the collection of quantitative information on their performance and to relate this information to the nanowire morphology. An efficiency of 12.8% (V_{oc}: 563 mV; J_{sc}: 33.5 mA cm^{-2}; fill factor (*FF*): 68.0%) was measured on planar Si with a doping level of 10^{15} cm^{-3},[24] which is in consistency with literature reports.[16,25,26] A slightly lower efficiency, 10.1%, was measured on EE SiNWs-based devices (V_{oc}: 550 mV; J_{sc}: 31.0 mA cm^{-2}; *FF*: 59.0%).

This result of EE SiNWs is significant in two respects. Firstly, the measured efficiency is among the highest reported for SiNWs generated by any preparation method (see Table 1). Secondly, the outstanding performance highlights the potential of nanowires. For instance it has been shown that a vertically aligned nanowire arrangement improves light absorption,[17–19,27] which presumably plays an important role in boosting the performance of EE SiNWs-based devices. Although the nanowire morphology is also predicted to improve charge separation, the relatively long charge-diffusion distance (> 100 μm at a doping level of 10^{15} cm^{-3}) makes such an effect a less important factor in this experiment.

By stark contrast, extremely modest efficiencies were measured on chemically grown SiNWs, the efficiencies being two orders of magnitude lower than those of EE SiNWs

[*] G. Yuan, K. Aruda, S. Zhou, A. Levine, J. Xie, Prof. Dr. D. Wang
Department of Chemistry, Boston College, Merkert Chemistry Center, 2609 Beacon St., Chestnut Hill, MA 02467 (USA)
Fax: (+1) 617-552-2705
E-mail: dunwei.wang@bc.edu
Homepage: http://www2.bc.edu/dunwei-wang

[**] This work was supported by a start-up fund and a RIG fund from Boston College; we thank NanoGreen solutions and Broadband Photonics for their gifts. We also thank Y. Lin for insightful discussions and S. Sheehan for his help with Figure 2.

Supporting information for this article is available on the WWW under http://dx.doi.org/10.1002/anie.201006617.

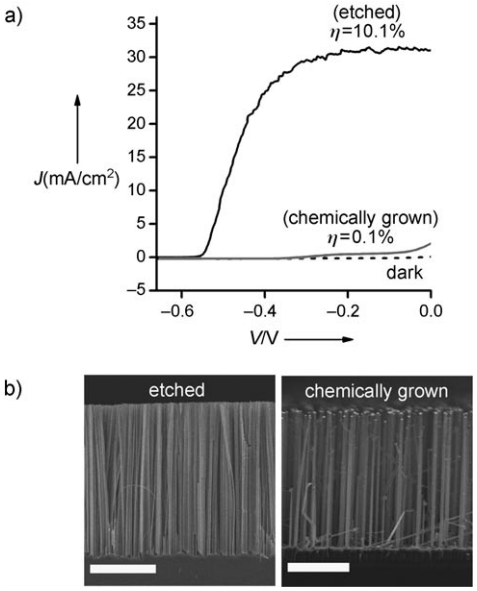

Figure 1. Comparison of SiNWs made by different methods. a) 10.1% energy conversion efficiency measured on electroless etched NWs; SiNWs of similar size, length, crystal structure, and doping level show 100 times lower performance. b) A side-by-side comparison of the NW morphologies. Note: although Au tips in the chemically grown NWs are seen in this picture, they are removed in the final devices. Scale bars: 5 μm.

(Figure 1). Note that by varying the doping levels, better performance on chemically grown SiNWs was measured ($\eta = 0.35\,\%$, doping level: 10^{18} cm^{-3}),[23] the performance nonetheless being on the same order of magnitude. To afford a more meaningful comparison, SiNWs of similar doping levels are compared herein, as shown in Figure 1. Considering that high efficiencies ($>10\,\%$) were determined for EE SiNWs by using the same technique, one can rule out the possibilities of measurement artifacts intrinsic to the nanowire morphologies that may be responsible for the low efficiencies. We also note that although higher efficiencies have been measured on individual chemically grown SiNWs, those measured on NW arrays are considerably lower than those of EE SiNWs or micrometer-scale Si wires (see Table 1). This result raises the question as to what limits the performance of chemically grown Si nanowires for energy conversion. We therefore compare microstructures of EE SiNWs and chemically grown ones to each other (Figure 1 b and Figure S1 in the Supporting Information). Evidentially, SiNWs made by these two methods show a remarkable resemblance in morphology, dimension, crystallinity, and doping level. As such, we conclude that the nanowire morphology is not intrinsically disadvantaged as far as the photovoltaic application is concerned. Studies of detailed charge behavior within SiNWs made by different methods are therefore needed to understand the origin of the poor performance by chemically grown ones.

Although the electronic properties of chemically grown SiNWs have been previously studied, these experiments were either performed in a field-effect-transistor configuration or focused on individual NWs.[4,10,28] Similar studies on vertically aligned NWs in an energy-conversion configuration are lacking. As a powerful analytical method, electrochemical impedance spectroscopy (EIS) is especially useful when a well-defined semiconductor/liquid interface is present in the target system.[29–31] By studying the response of the system under alternating current (AC) perturbations of different frequencies, various electronic states in the semiconductor can be identified quantitatively or quasi-quantitatively. Widely employed in understanding battery electrodes and many other systems,[32–35] the application of EIS in studying SiNWs in an energy conversion setting is scarce.

When immersed in the electrolyte, an inversion layer forms near the semiconductor/liquid interface as a result of band bending. This layer, also known as the space-charge region, is the focus of our subsequent discussions; in the detailed quantitative analysis, the characteristics of the Helmholtz double layer, redox transport in the electrolyte solution, and the series resistance were included. As the nature of these factors is well understood (such as using a Warburg impedance component to simulate the redox transport in the solution[36]), we limit the following discussions to the components that concern the semiconductor characteristics, that is, the space-charge region within the SiNWs. The band bending in the SiNWs and the corresponding equivalent electrical circuits are drawn in Figure 2.

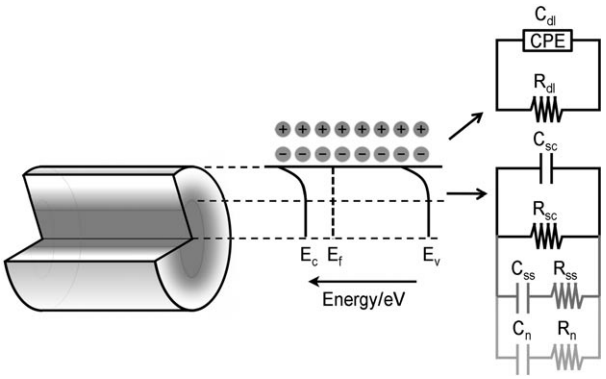

Figure 2. Schematic of the electronic structure of the interface between a SiNW and the electrolyte. An electrical equivalent circuit that facilitates the data analysis of the impedance spectra is shown on the right.

We first examined the Bode plots of EE SiNWs, where the overall impedance (Z) is plotted against the frequencies (f) of the AC perturbations. When $f < 100$ Hz, $|Z|$ is dominated by the resistance of the system, which changes negligibly with the increase of f. On the other hand, when $f > 5$ kHz, the capacitive nature of the space-charge region begins to manifest itself, hence resulting in a single time constant in the phase Bode plot (see the Supporting Information) and a linear tail in the logarithm-scale impedance Bode plot ($|Z| \propto 1/f$), Figure 3 a. The good fitting with a slope of -1 in the logarithm scale for the high frequency range in Figure 3 a signifies that in this frequency range the overall impedance is dominated by that of the space-charge region. A similar conclusion is reached by studying the Nyquist plot: as shown in Figure 3 b, between $f = 100$ kHz and 147 Hz, a semicircle is

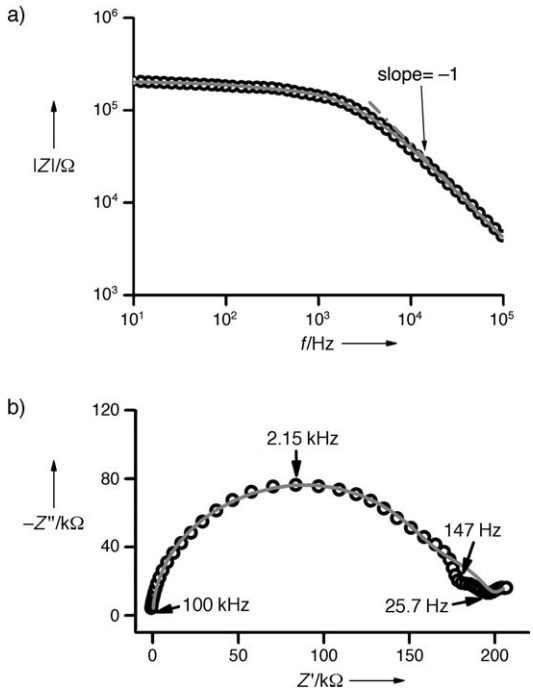

Figure 3. EIS data of EE SiNWs at 0 V. a) Bode plot; a linear fitting in the high-frequency range with a slope of −1 is obtained. b) Nyquist plot. Both plots: open circles: experimental data, solid lines: simulated data; several randomly chosen frequencies are labeled in (b) to provide information on the frequency dependence.

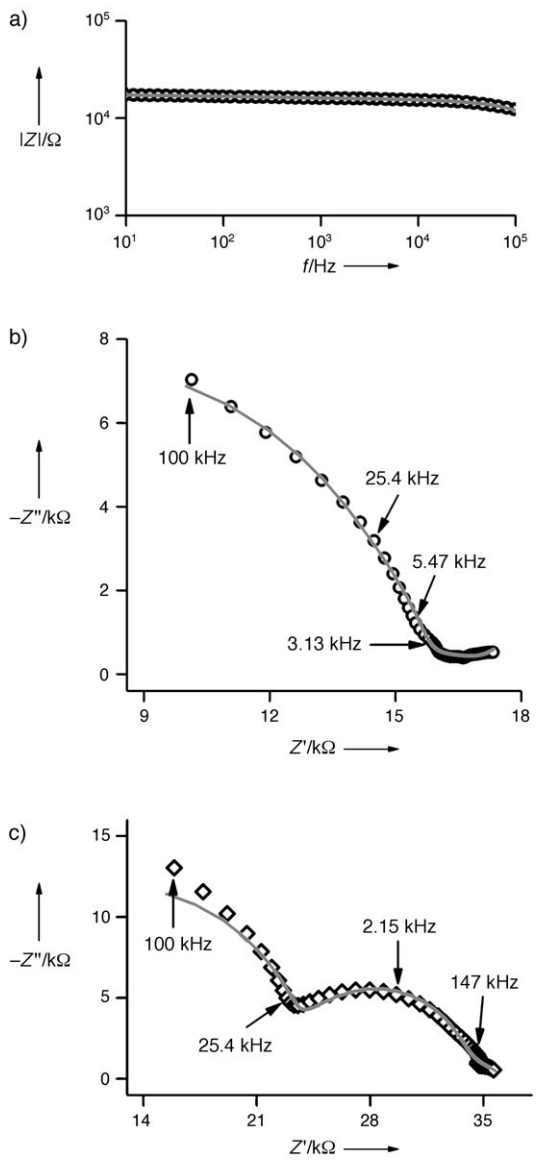

Figure 4. EIS data of chemically grown SiNWs at 0 V. a) Bode plot; b) Nyquist plot. c) To better manifest the arc corresponding to the space-charge region, a set of data obtained at 0.4 V applied potential, under which condition the space-charge region is better developed, is added to this plot.

fully developed, thus suggesting the capacitive nature of the impedance in this frequency range. It is important to note, however, that the semicircle in Figure 3b contains information on the space-charge region and that of the semiconductor/liquid interface.

An excellent correlation (fitting error: $<6\,\%$) was shown when simulated data obtained by using the electrical equivalent circuit (EEC) in Figure 2 were compared with the experimental Bode plot and Nyquist plot, as shown in Figure 3. Note that as a result of surface imperfections such as structural defects or undesired chemisorption, a capacitor/resistor (C_{ss}/R_{ss}) combination in parallel to those that represent the capacitance and the resistance of the space-charge region was necessary to obtain the presented fitting result. The deviation below 100 Hz may be caused by the complex nature of the electrochemical processes at a high-surface-area interface, where the EEC method fails to fully account for the observed details. Understanding this portion of data will require further study and is out of the scope of the current work as we primarily focus on the higher frequency regions to understand the electronic properties within the semiconductor. The parameters used for the fitting of the Nyquist plot provide critical quantitative information on the space-charge region, including the capacitance, the resistance, and the charge concentration. At 0 V applied potential, the values are 3.97×10^{-10} F (capacitance) and $1.62\times10^{5}\ \Omega$ (resistance), which change to 3.00×10^{-10} F and $5.30\times10^{5}\ \Omega$ at 0.4 V (complete set of data: see the Supporting Information). Importantly, the capacitance that may be ascribed to that of the surface states remained constant as the applied potentials were varied, thus further validating our simulation methodology. Following the Mott–Schottky relation [Eq. (1)]:

$$C_{SC}^{-2}=\frac{2}{A^2 q\varepsilon\varepsilon_0 N_D}\left(V-V_{fb}-\frac{kT}{q}\right) \qquad (1)$$

(where ε is the permittivity of free space; ε_0 is the dielectric constant of silicon; V is the applied potential; V_{fb} is the flatband potential; N_D is the dopant density of silicon; A is the surface area of the electrode; k is the Boltzmann constant, and T is the temperature), we obtained a flatband potential (V_{fb}) of 0.529 V, Figure 5. Without excluding the capacitance caused by the surface states, a flatband potential of 0.508 V

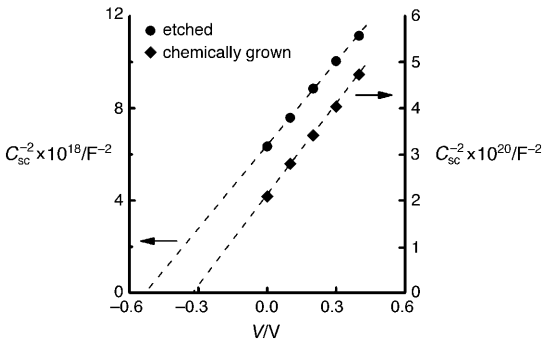

Figure 5. Mott–Schottky plot of chemically grown and EE SiNWs.

would be obtained, a misinformation that may weaken efforts for device optimization.

When similar experiments were performed on chemically grown SiNWs, drastically different results were obtained (Figure 4). Firstly, in the low-frequency region, the impedance is approximately 10 times lower than that of EE SiNWs, despite the fact that extra caution was taken to passivate the surface of the supporting substrate by using Al_2O_3 (see the Experimental Section).[23] Secondly, although the general trend that $|Z|$ decreases as f increases is followed, it significantly deviates from $|Z| \propto 1/f$ (Figure 4a). This result suggests that charge-transfer channels other than that through the space-charge region and the surface states exist; these channels seriously undermine the capacitive nature of the space-charge region. Quantitative analysis by fitting the Bode plot and Nyquist plot, Figure 4, resulted in an additional capacitor/resistor (C_n/R_n) component (Figure 2). Thirdly, the high-frequency end of the Nyquist plot is reminiscent of a tail of a capacitive arc, hence indicating that fast-kinetic electronic processes take place in the chemically grown SiNWs. Owing to instrumentation limitations, we were unable to probe the process at $f > 100$ kHz. From the Mott–Schottky plot using the space-charge region capacitance calculated from the Nyquist plot fitting, we obtained the flatband potential of chemically grown SiNWs as 0.323 V. This value is lower than the one for EE SiNWs by 0.206 V and may be caused by Fermi level pinning because of the additional states.

Although the exact nature and the origin of the additional states are unclear, it is the first time that such states have been quasi-quantitatively identified. As the effects of similar defects are not observed on SiNWs of comparable dimension, crystallinity, and doping level, but different preparation technique (electroless etching), we hypothesize that this type of defects result from the synthetic step. This understanding is particularly important, given the widely varying conditions for SiNWs preparation.[3–5] For example, the early research on electronic properties of SiNWs in a field-effect-transistor configuration almost entirely focused on SiNWs grown chemically by SiH_4 chemistry at relatively low temperatures (ca. 500 °C or lower), under which conditions SiNWs grow fast and are of low defect densities. Comparably fewer studies of vertically aligned SiNWs that were used for solar energy conversion were conducted by using the same chemistry. Instead, SiNWs were grown at higher temperatures, which are known to introduce Au impurities, thus creating deep level traps.[37] It has also been suggested that growth seeds other than Au should be used.[38,39] An important contribution to this understanding is our observation that nanowire morphology deserves significant research attention and that the focus should be on growth chemistry. We also emphasize that the performance of SiNWs for solar energy conversion needs to be cautiously compared by taking into account the preparation methods; otherwise misleading conclusions may be drawn.

Experimental Section

SiNW Synthesis: Electroless etched SiNWs were prepared following a reported method.[20] An n-type Si (100) substrate (ca. 2.7–4 Ω cm, Wafternet) was cleaned with acetone, methanol, and isopropanol sequentially. The substrate was subsequently oxidized in H_2O_2/H_2SO_4 1:3 at 90 °C for 10 min to remove heavy metals and organic species, and was then rinsed with deionized (DI) water. Finally, the cleaned substrate was immersed into an $HF/AgNO_3$ solution (4.6 M HF and 0.02 M $AgNO_3$) for 30–45 min at 50 °C to produce SiNWs. Chemically grown SiNWs were synthesized by a method previously reported by us.[23] The growth was carried out in a homebuilt chemical vapor deposition apparatus with automatic flow and pressure controls. Doping was accomplished and controlled by varying the SiH_4/PH_3 ratio during the synthesis. Doping levels were calculated from four-probe resistance measurements.

Photoelectrode fabrication: After etching in 5% HF for 2 min and thorough rinsing with DI water, the electroless etched SiNWs were used directly for electrode fabrication. Ohmic contact was made by applying a Ga/In eutectic and by fixing tinned copper wire with Ag epoxy (SPI supplies). The entire sample was sealed with non-conductive hysol epoxy (Loctite), leaving the front-side SiNWs arrays exposed. The chemically grown SiNWs were subjected to a series of post-growth treatments to achieve Al_2O_3 passivation, as detailed in our previous work.[23] The electrical contact was made as described above.

Photoelectrochemical and Impedance Measurements: The photoelectrochemical measurements were conducted using a CHI 604C Potentiostat/Galvanostat in a three-electrode configuration. A platinum wire in a Luggin capillary was used as the reference electrode and a platinum mesh served as the counter electrode. The methanolic electrolyte solution consisted of 200 mM dimethylferrocene (Me_2Fc) (97%, Alfa Aesar), 0.1 mM Me_2FcBF_4, and 1.00 M $LiClO_4$ (> 99%, Fisher). All reagents were used as received without further purification except $Me_2Fc^+BF_4^-$, which was synthesized in-house.[23] For all data reported here, simulated sunlight (100 mW cm^{-2}, AM 1.5, Oriel 96000) was used as the light source. The current density versus potential (J–V) measurements were conducted at a scan rate of 10 mV s^{-1}. Voltage corrections were performed to eliminate the influence of series resistance and concentration overpotential. The impedance measurements were performed using the same cell configuration and instrument as the photoelectrochemical measurements coupled with a frequency analyzer. The solution contained the same chemicals except that the Me_2FcBF_4 concentration was increased to 1 mM. This change was found to give highly reproducible data. The impedance measurements were performed with 5 mV amplitude modulation on a reverse direct current bias between 0 and 0.4 V versus Nernst solution potential in the dark; the frequency range was between 10 and 100 kHz. The EIS spectra fitting was carried out using the software associated with the CHI instrument. J–V measurements in the dark were repeated before and after each applied potential of impedance measurements to ensure that no

irreversible changes occurred to the photoelectrode under investigation.

Received: October 21, 2010
Published online: February 2, 2011

Keywords: chemical vapor deposition · electrochemical impedance spectroscopy · energy conversion · silicon · solar cells

[1] B. M. Kayes, H. A. Atwater, N. S. Lewis, *J. Appl. Phys.* **2005**, *97*, 114302.
[2] A. I. Hochbaum, P. Yang, *Chem. Rev.* **2010**, *110*, 527 – 546.
[3] V. Schmidt, J. V. Wittemann, U. Gosele, *Chem. Rev.* **2010**, *110*, 361 – 388.
[4] V. Schmidt, J. V. Wittemann, S. Senz, U. Gösele, *Adv. Mater.* **2009**, *21*, 2681 – 2702.
[5] A. Levine, G. Yuan, J. Xie, D. Wang, *Sci. Adv. Mater.* **2010**, *2*, 463 – 473.
[6] B. Tian, X. Zheng, T. J. Kempa, Y. Fang, N. Yu, G. Yu, J. Huang, C. M. Lieber, *Nature* **2007**, *449*, 885 – 889.
[7] M. D. Kelzenberg, S. W. Boettcher, J. A. Petykiewicz, D. B. Turner-Evans, M. C. Putnam, E. L. Warren, J. M. Spurgeon, R. M. Briggs, N. S. Lewis, H. A. Atwater, *Nat. Mater.* **2010**, *9*, 239 – 244.
[8] M. C. Putnam, S. W. Boettcher, M. D. Kelzenberg, D. B. Turner-Evans, J. M. Spurgeon, E. L. Warren, R. M. Briggs, N. S. Lewis, H. A. Atwater, *Energy Environ. Sci.* **2010**, *3*, 1037 – 1041.
[9] J. R. Maiolo, B. M. Kayes, M. A. Filler, M. C. Putnam, M. D. Kelzenberg, H. A. Atwater, N. S. Lewis, *J. Am. Chem. Soc.* **2007**, *129*, 12346 – 12347.
[10] M. D. Kelzenberg, D. B. Turner-Evans, B. M. Kayes, M. A. Filler, M. C. Putnam, N. S. Lewis, H. A. Atwater, *Nano Lett.* **2008**, *8*, 710 – 714.
[11] L. Tsakalakos, J. Balch, J. Fronheiser, B. A. Korevaar, O. Sulima, J. Rand, *Appl. Phys. Lett.* **2007**, *91*, 233117.
[12] A. P. Goodey, S. M. Eichfeld, K. K. Lew, J. M. Redwing, T. E. Mallouk, *J. Am. Chem. Soc.* **2007**, *129*, 12344 – 12345.
[13] E. C. Garnett, P. Yang, *J. Am. Chem. Soc.* **2008**, *130*, 9224 – 9225.
[14] O. Gunawan, S. Guha, *Sol. Energy Mater. Sol. Cells* **2009**, *93*, 1388 – 1393.
[15] S. W. Boettcher, J. M. Spurgeon, M. C. Putnam, E. L. Warren, D. B. Turner-Evans, M. D. Kelzenberg, J. R. Maiolo, H. A. Atwater, N. S. Lewis, *Science* **2010**, *327*, 185 – 187.
[16] J. R. Maiolo, H. A. Atwater, N. S. Lewis, *J. Phys. Chem. C* **2008**, *112*, 6194 – 6201.
[17] L. Hu, G. Chen, *Nano Lett.* **2007**, *7*, 3249 – 3252.
[18] L. Tsakalakos, J. Balch, J. Fronheiser, M.-Y. Shih, S. F. LeBoeuf, M. Pietrzykowski, P. J. Codella, B. A. Korevaar, O. V. Sulima, J. Rand, A. Davuluru, U. Rapol, *J. Nanophotonics* **2007**, *1*, 013552.
[19] E. Garnett, P. Yang, *Nano Lett.* **2010**, *10*, 1082 – 1087.
[20] K. Peng, Y. Xu, Y. Wu, Y. Yan, S.-T. Lee, J. Zhu, *Small* **2005**, *1*, 1062 – 1067.
[21] K. Hagedorn, C. Forgacs, S. Collins, S. Maldonado, *J. Phys. Chem. C* **2010**, *114*, 12010 – 1201777.
[22] K.-Q. Peng, X. Wang, X.-L. Wu, S.-T. Lee, *Nano Lett.* **2009**, *9*, 3704 – 3709.
[23] G. Yuan, H. Z. Zhao, X. H. Liu, Z. Hasanali, Y. Zou, A. Levine, D. Wang, *Angew. Chem.* **2009**, *121*, 9860 – 9864; *Angew. Chem. Int. Ed.* **2009**, *48*, 9680 – 9684.
[24] Concentration-induced overpotentials and series resistance losses were calculated and compensated for the efficiency calculations.
[25] J. F. Gibbons, G. W. Cogan, C. M. Gronet, N. S. Lewis, *Appl. Phys. Lett.* **1984**, *45*, 1095 – 1097.
[26] M. L. Rosenbluth, C. M. Lieber, N. S. Lewis, *Appl. Phys. Lett.* **1984**, *45*, 423 – 425.
[27] J. Li, H. Yu, S. M. Wong, X. Li, G. Zhang, P. G.-Q. Lo, D.-L. Kwong, *Appl. Phys. Lett.* **2009**, *95*, 243113.
[28] T. J. Kempa, B. Z. Tian, D. R. Kim, J. S. Hu, X. L. Zheng, C. M. Lieber, *Nano Lett.* **2008**, *8*, 3456 – 3460.
[29] I. D. Raistrick, *Annu. Rev. Mater. Sci.* **1986**, *16*, 343 – 370.
[30] M. C. A. Fantini, W.-M. Shen, M. Tomkiewicz, J. P. Gambino, *J. Appl. Phys.* **1989**, *65*, 4884 – 4890.
[31] G. Oskam, P. M. Hoffmann, J. C. Schmidt, P. C. Searson, *J. Phys. Chem.* **1996**, *100*, 1801 – 1806.
[32] W. Weppner in *Solid State Electrochemistry* (Ed.: P. G. Bruce), Cambridge University Press, Cambridge, **1995**, pp. 199 – 228.
[33] R. Ruffo, S. S. Hong, C. K. Chan, R. A. Huggins, Y. Cui, *J. Phys. Chem. C* **2009**, *113*, 11390 – 11398.
[34] C. Ho, I. D. Raistrick, R. A. Huggins, *J. Electrochem. Soc.* **1980**, *127*, 343 – 350.
[35] D. D. Macdonald, *Electrochim. Acta* **2006**, *51*, 1376 – 1388.
[36] M. E. Orazem, B. Tribollet, *Electrochemical Impedance Spectroscopy*, Wiley, Hoboken, NJ, **2008**.
[37] W. M. Bullis, *Solid State Electron* **1966**, *9*, 143 – 168.
[38] B. M. Kayes, M. A. Filler, M. C. Putnam, M. D. Kelzenberg, N. S. Lewis, H. A. Atwater, *Appl. Phys. Lett.* **2007**, *91*, 103110.
[39] Y. W. Wang, V. Schmidt, S. Senz, U. Gosele, *Nat. Nanotechnol.* **2006**, *1*, 186 – 189.

